Ready to Navigate!
A Methodology for the Estimation of the Time-to-First-Fix

FEMA photo by Patsy Lynch

Estimating and comparing the various GNSS signals' time-to-first-fix is an excellent tool for evaluating the design trades made on GNSS signal structures and a particularly important feature for general users in the mass market. This column describes the various factors that contribute to delays in a receiver's initial position fix and proposes a methodology for estimating time-to-first-fix for various signals and receiver start conditions.

MARCO ANGHILERI, MATTEO PAONNI, STEFAN WALLNER, JOSÉ-ÁNGEL ÁVILA-RODRÍGUEZ, BERND EISSFELLER
INSTITUTE OF GEODESY AND NAVIGATION, UNIVERSITY FAF MUNICH, GERMANY

After three decades of increasingly widespread use, satellite navigation-based services have changed significantly, especially for general users in the mass market. New technology enablers such as assisted GPS (A-GPS), the use of massively parallel correlation, and the application of advanced positioning techniques have significantly enhanced the time-to-first-fix (TTFF) and sensitivity of today's receivers.

Although these techniques have increased satisfaction for end users, they could partially mask many particular differences expressed among the various GNSS signals, today and in the future.

These new signals contain many innovations, including the use of longer spreading codes, new modulation techniques, and new navigation message structures using channel-coding techniques.

With such a wide variety of signals, it is essential to define criteria that enable us to understand the main differences among the signals, as well as under which conditions one would perform better than others and their relative suitability for particular applications.

Among the different performance metrics, estimating and comparing the various signals' TTFF is an excellent tool for evaluating the design trades made on GNSS signal structures, especially those concerning spreading codes and navigation messages.

In this article we propose a methodology to account for and evaluate what happens in a conventional receiver

"behind the scenes," from the very first moment the receiver is switched on, until it is "ready to navigate".

After presenting a theory that may be applied to any GNSS signal, we discuss simulation results obtained with some GPS and Galileo signals. Our proposed approach can be seen as an extension of the methodology described in the article by J. K. Holmes *et alia*, listed in the Additional Resources section near the end of this column, where the results are computed for a confidence level of 95 percent.

Definition of TTFF

With the expression time-to-first-fix, we generally refer to the time needed by the receiver to perform the first position fix, starting from the moment it is switched on.

Usually we distinguish among three different TTFF scenarios, depending on the particular status of the receiver when it is started. We refer to cold, warm, or hot starts according to the availability and validity of the data required for computing the navigation solution (satellite almanac and ephemeris parameters, send time of the received signal, previously stored PVT solutions). These three cases can be described as follows:

- **Cold Start:** No data is stored in the receiver; however, the position solution can be calculated by a full sky search without the use of any almanac data. *For the first position fix, clock correction and ephemeris data (CED), together with a GNSS time reference (GST) must be retrieved.*
- **Warm Start:** Valid ephemeris and clock corrections are stored in the device and the *receiver just needs to retrieve the GST information from the navigation message.*
- **Hot Start:** The warm start conditions apply; in addition, accurate position and clock error are known. *The position solution can be computed without any information from the navigation message.*

In addition to the availability of navigation data, TTFF performance depends on the number of visible satellites and the strength of the received signals.

In this study, we performed all our analyses with three baseline assumptions: (1) received signals have high enough C/N_0 (e.g. no bit errors), (2) the number of visible satellites is always sufficient to allow the receiver to perform a first position fix within the standard accuracy requirements; and (3) the receiver uses parallel processing on all the signals coming from the different satellites, as is common in a state-of-the-art receiver today. Under these three conditions the TTFF equals the time needed to process one of the signals coming from the different satellites.

In the following sections we present a methodology for the computation of a 95 percent probability of TTFF. This method may be applied to any GNSS signal.

The approach also may be seen as a generalization of J. K. Holmes' method, where the TTFF is subdivided into different contributions, each of which may be estimated separately and the combination of which produces the final result.

Contributions to the TTFF

The individual contributions to the TTFF trace to the individual tasks performed by the receiver from the moment it is switched on, until the first valid position solution is reported.

Depending on the start condition, the TTFF can be described as follows:

$$TTFF_{cold} = T_{warm-up} + T_{acq} + T_{track} + T_{CED+GST} + T_{PVT} \quad (1)$$

$$TTFF_{warm} = T_{warm-up} + T_{acq} + T_{track} + T_{GST} + T_{PVT} \quad (2)$$

$$TTFF_{hot} = T_{acq} + T_{track} \quad (3)$$

where:

$T_{warm-up}$: receiver warm-up time
T_{acq}: acquisition time
T_{track}: settling time for code and carrier tracking
$T_{CED+GST}$: navigation data read time (clock correction and ephemeris data or CED plus the GNSS System Time, GST)
T_{GST}: time to retrieve the system time reference
T_{PVT}: time to compute the navigation solution

The receiver warm-up time includes all software and hardware initializations carried out from the first moment the equipment is switched on. Because the performance obviously depends strongly on the GNSS receiver's technology, in this case for our purposes we assumed this warm-up time to be two seconds for all receivers.

The time to compute the navigation solution is mainly due to the initialization of the algorithms for the positioning solution, typically by a Kalman filter or least squares method. Especially in the cold start case, with no prior knowledge of the user position, the algorithms are initialized supposing the user to be located in the center of the Earth.

Because of this assumption the positioning algorithm requires some iterations to converge to the positioning solutions. The time needed for these iterations is called T_{PVT}. For a warm start, a very approximate positioning solution can be used, and thus the T_{PVT} contribution becomes smaller. Finally, in the case of a hot start, the time is considered negligible.

Acquisition Time

We turn our discussion to the main contributors of the overall TTFF calculation and the theory necessary to compute T_{acq}, T_{track}, $T_{CED+GST}$, and T_{GST}.

We treat the acquisition process as a detection problem, usually performed in a navigation receiver by measuring the complex amplitude of the correlator's output. The test statistic is thus defined and compared with a predefined fixed threshold, indicating whether the signal sought is present.

We set the threshold in order to minimize the probability of false alarms while maintaining a high probability of detection. As shown in the chapter on GPS receivers by A. J. Van Dierendonck (see Additional Resources), during the coherent integration, a number *M* of intermediate frequency (IF) in-phase (I) and quad-phase (Q) prompt correlator samples are

each summed coherently, squared, and then added together, resulting in the following expression:

$$y_C = \left(\sum_{i=1}^{M} I_i \right)^2 + \left(\sum_{i=1}^{M} Q_i \right)^2 \qquad (4)$$

where y_C represents the squared summation of the samples.

The number M of samples summed in the coherent integration is determined using a coherent integration time T.

The final test statistic, y_{NC}, is the non-coherent summation of K consecutive coherent integrations after squaring:

$$y_{NC} = \sum_{j=1}^{K} y_{C_j} = \sum_{j=1}^{K} \left[\left(\sum_{i=1}^{M} I_i \right)^2 + \left(\sum_{i=1}^{M} Q_i \right)^2 \right]_j \qquad (5)$$

We note that Equation (5), commonly known as dwell time, is the product of T and K and is the time needed to perform the detection, consisting of coherent and non-coherent integrations. As explained in the article by A. J. Van Dierendonck cited in Additional Resources, the signal detection problem is essentially a statistical exercise based on a hypothesis test. Thus, defining TH as the test threshold, for the hypothesis test we have:

- $y_{NC} > TH$ under the hypothesis H_1 (signal is present)
- $y_{NC} < TH$ under the hypothesis H_0 (signal is not present)

Statistical Method

The probability density functions of the test statistics under the hypotheses H_1 and H_0, as discussed in the article by J. A. Ávila-Rodríguez, are defined as follows:

$$p(y_{NC} | H_1) = \frac{1}{2} \left(\frac{y_{NC}}{K\alpha} \right)^{\frac{1}{2}(K-1)} \cdot e^{-\frac{1}{2}(y_{NC} - K\alpha)} \cdot I_{K-1}\left(\sqrt{K\alpha y_{NC}} \right), y_{NC} \geq 0 \quad (6)$$

and

$$p(y_{NC} | H_0) = e^{-\frac{y_{NC}}{2}} \sum_{n=0}^{K-1} \frac{1}{2^n (n-1)!} y_{NC}^{n-1}, y_{NC} \geq 0 \qquad (7)$$

where $I_{K-1}(x)$ is the modified Bessel function of the first kind, and α is the post-correlation signal-to-noise-ratio, defined in Equation (8):

$$\alpha = 2TC / N_0 \qquad (8)$$

As is well known, the acquisition is performed following a two-dimensional search in frequency and code delay. We need to define the search space and search strategy in order to correctly estimate the acquisition time.

The search space has to cover the full range of uncertainty of the code delay and carrier Doppler shift. With respect to the code delay search space, the range of the possible offset values depends on the specific code that must be acquired.

The Doppler frequency shift search space, fixed to a maximum possible Doppler shift, mainly depends on the carrier frequency of the signal to be acquired, on the particular orbital characteristics of the associated constellation, and the speed of the user that is receiving it.

We assume a one-half code chip resolution for the code delay dimension of the search space. With respect to the Dop-pler shift resolution, the width of the Doppler bin, the fundamental unit here, depends mainly on the integration time, and can be defined as follows:

$$\delta f = 2/3T \qquad (9)$$

In order to perform simulations, the coherent integration time, T, as well as the number of non-coherent summations, K, must be fixed for all the signals under study. In order to keep the acquisition time as short as possible and maintain the hypothesis of a "high enough" C/N_0, we fix K at 1 for all the cases. We consider T for all signals as the length of one code period. **Table 1** lists the values chosen for each of the various signals.

Consequently, we calculate the search space dimension as:

$$N = N_f N_T = \frac{\Delta f}{\delta f} \frac{\Delta T}{\delta t} \qquad (10)$$

where $\Delta f = 2 f_d^{MAX}$ is the range of frequency values to be searched. ΔT is the range of code shift values to be searched and also equals the length of the code, while δf and δt are the frequency and code shift bin dimensions, respectively.

Under these hypotheses we calculate the search space dimensions for the five signals analyzed. The results are reported in **Table 2**.

Because massively parallel correlators or a fast Fourier transform (FFT) approach (or both) are used in modern GNSS receivers, the number of dwell times needed to span the full search space decreases. If P_f and P_T are representing the number of frequency and code bins that are searched in parallel, then the total number of parallel correlations needed in the acquisition process is:

$$N_P = \frac{N}{P} = \frac{N_f N_T}{P_f P_T} = N_{P_f} N_{P_T} \qquad (11)$$

where $P = P_f P_T$ is the total number of bins that are searched in parallel in both code and frequency, and $N_p = N_{pf} N_{pT}$ is the total number of parallel correlations that actually contribute to the acquisition time.

In the cases of both warm and hot starts, we consider a reacquisition pro-

Signal	T [ms]
Galileo E1-B	4
Galileo E5a-I	1
GPS L1 C/A	1
GPS L1C	10
GPS L5-I5	1

TABLE 1. Coherent integration time values

Signal	N_F	δf [Hz]	N_T	δt [chips]
Galileo E1-B	50	167	8184	0.5
Galileo E5a-I	10	667	20460	0.5
GPS L1 C/A	15	667	2064	0.5
GPS L1C	147	67	20460	0.5
GPS L5-I5	11	667	20460	0.5

TABLE 2. Search space dimensions

Signal	Cold Start	Warm Start	Hot Start
Galileo E1-B	2.07	0.92	0.10
Galileo E5a-I	0.26	0.15	0.03
GPS L1 C/A	0.04	0.02	0.01
GPS L1C	41.02	14.62	1.06
GPS L5-I5	0.29	0.16	0.03

TABLE 3. $T_{acq}(95\%)[s]$ – Maximum search

Signal	Cold Start	Warm Start	Hot Start
Galileo E1-B	1.13	0.48	0.05
Galileo E5a-I	0.13	0.08	0.02
GPS L1 C/A	0.02	0.01	0.003
GPS L1C	33.21	8.64	0.54
GPS L5-I5	0.15	0.08	0.02

TABLE 4. $T_{acq}(95\%)[s]$ – Serial search

Signal	Cold Start	Warm Start	Hot Start
Galileo E1-B	0.04	0.03	0.02
Galileo E5a-I	0.03	0.02	0.01
GPS L1 C/A	0.01	0.01	0.003
GPS L1C	0.36	0.28	0.22
GPS L5-I5	0.03	0.02	0.01

TABLE 5. $T_{acq}(95\%)[s]$ – Hybrid search

cess. In these cases the search space is reduced from that used for a cold start. The code shift dimension remains unchanged, while fewer Doppler bins need to be accounted for.

For the purpose of this work, the dynamic variation rate for a signal transmitted at L-band frequencies has been estimated at one hertz per second. Therefore, if after 10 minutes a signal must be reacquired, for example, then the Doppler range to be scanned would be ±600 Hz.

Following the discussion in the article by D. Borio *et alia*, we considered three main search strategies: serial search, maximum search, and hybrid search. Details on these search techniques can be found under Additional Resources, in the articles by A. Polydoros et alia, G. E. Corazza, and H. Mathis *et alia*, respectively.

The expressions for probability of detection and probability of false alarm during the acquisition process previously introduced are independent of the search strategy, because we evaluate them within a single cell of the search space.

We build on the expressions presented in the articles by D. Borio *et alia* and D. Borio for system detection and false alarm probabilities in order to evaluate of the acquisition time for the various search strategies. The system detection probabilities for the three search strategies previously introduced are the following:

$$p_{D,Serial} = \frac{1}{N_p} \frac{1 - [1 - p_{fa}]^{N_p}}{p_{fa}} p_d \qquad (12)$$

$$p_{D,Maximum} = \int_{TH}^{\infty} [1 - p_{fa}]^{N_p - 1} p(y_C \mid H_1) dy_C \qquad (13)$$

$$p_{D,Hybrid} = \frac{1}{N_{p_f}} \frac{1 - [1 - p_{fa}]^{N_p}}{1 - [1 - p_{fa}]^{N_{p_T}}} \int_{TH}^{\infty} [1 - p_{fa}]^{N_{p_T} - 1} p(y_C \mid H_1) dy_C \qquad (14)$$

where p_d and p_{fa} are the single cell probabilities of detection and false alarm.

The acquisition decision is made taking into account the whole search space; however, the system probabilities just described are also extremely important, especially in calculating the time needed to perform the acquisition process. These probabilities are defined under the two assumptions, (a) that the single cell probabilities are verified only for one cell of the search space, and (b) that the random cells are statistically independent.

Let us now derive the expression for the acquisition time for the easiest case, corresponding to the maximum search strategy. In this case, the mean time to sweep the whole search space is given by J. K. Holmes (2007) in the following expression:

$$\overline{T}_{SW} = T_D N_p + k_p T_D \cdot N_p (p_{fa})_p \qquad (15)$$

where T_D is the total dwell time, and N_p is the search space dimension previously defined, while $(p_{fa})_p$ is the effective false alarm probability that takes into account the fact that more cells are searched in parallel, defined as follows:

$$(p_{fa})_p = 1 - (1 - p_{fa})^P \qquad (16)$$

Moreover, in Equation (15) $k_p T$ is the so-called penalty time needed to verify that the false alarm is really a false alarm and not a true lock point. For the simulations in this work, $k_p = 3$.

Using the mean sweep time, we define the probability of acquisition after n searches of seconds through the search space as

$$P_{acq}(n\overline{T}_{SW}) = 1 - (1 - P_D)^n \qquad (17)$$

where P_D is the system probability of detection for different search strategies. Therefore, if the required probability of acquisition is higher than the system probability of detection, more than one sweep of the search space is needed. By fixing a given probability of acquisition, the corresponding time needed to acquire the signal with that probability can be calculated.

Statistical Results

In the simulations we performed, we assumed 30,000 correlators for all the three search strategies, common in today's navigation receivers. Moreover, we assumed a single cell detection probability of 0.9 and a single cell false alarm probability of 10^{-3}.

The acquisition time for a 95 percent confidence level has been calculated for the five GNSS signals, applying the three different search techniques discussed earlier to each of the cold, warm and hot start cases. Thus, we considered nine different simulation scenarios for each signal.

We selected a reacquisition time of 30 minutes and 60 seconds, for a warm and hot start, respectively. The results of the simulations for the T_{acq} (95%) are listed in **Tables 3**, **4**, and **5** for maximum, serial, and hybrid search strategies, respectively.
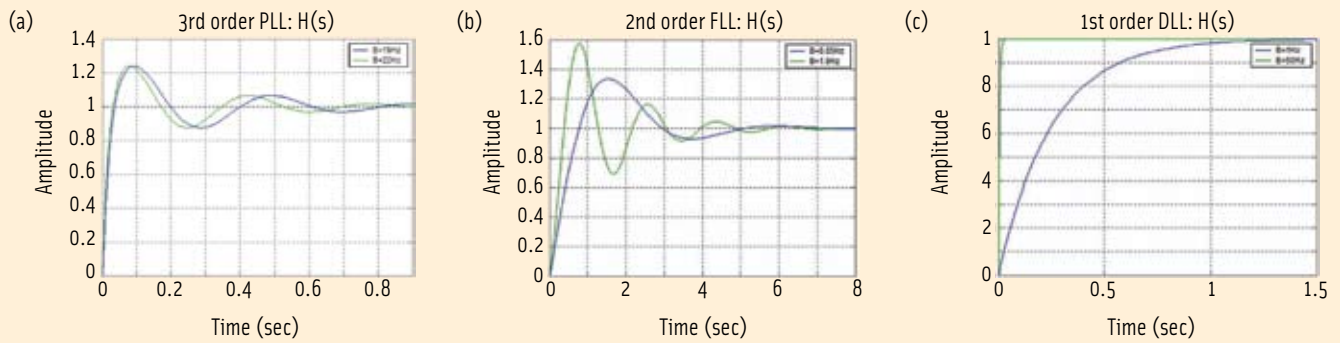
FIGURE 1 Step response of the tracking loops in a GNSS receiver. a) PLL b) FLL c) DLL (from the article by J-H Won *et alia*.)

In the case of hybrid approach, the frequency domain is searched using an FFT-based method, while a maximum search is used in the code dimension.

The acquisition time in the case of a "high-enough" signal to noise ratio is quite short. The only exception is represented by GPS L1C, where the coherent integration time for L1C is assumed to be 10 milliseconds, while the search space is the widest, as shown in Table 2.

As expected, the best performance is achieved for GPS L1 C/A, due to its shortest code and coherent integration time. Galileo E5a-I and GPS L5-I5 show similar results, while slightly longer times are needed to acquire Galileo E1-B, because a coherent integration time of four milliseconds has been considered.

Simulations for the acquisition time in conditions of lower signal to noise ratio can be found in the article by M. Paonni *et alia* (Additional Resources).

Initialization of Tracking Loops

The receiver's tracking loop (PLL, FLL, and DLL) require, before entering their stable region, a transient time estimated by studying their step response. Even if this time is dependent on the chosen loop bandwidths, generally the settling times of PLL and DLL are significantly shorter compared to the time required by the FLL, as shown in **Figure 1**.

As shown in the Figure1(b), the FLL loop is of second order, resulting in a curve that oscillates for a few seconds before reaching the steady state, where the amplitude of the response equals the amplitude of the input step. In accordance with the overall approach followed in this work, we read the time value when the curve's amplitude remains between 0.95 and 1.05.

In agreement with the results in J. K. Holmes *et alia*, a value of 4.8 seconds for the cold and warm start cases has been chosen, while in case of a hot start, this time contribution reduces significantly to an assumed 0.5 seconds.

Frame Synchronization

In today's GNSS navigation messages, data is arranged in a multi-level structure composed of *frames*, *subframes*, *messages*, *pages*, and *words*. See the sidebar entitled "Navigation Message Architecture and Terminology" for a brief description of the generic structure of navigation messages.

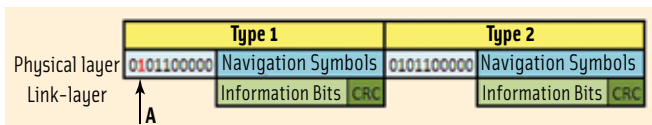A common feature of the various types of messages is that,

FIGURE 3 Generic structure of two consecutive pages

after retrieving the navigation bits, a validity check, such as a *cyclic redundancy check* (CRC), is performed. Considering the number of bits to which this check applies, together with the field containing the checksum, the block of navigation symbols obtained by encoding these bits is called a *page*.

Usually the page contains also a known sequence of symbols located at the beginning and called the *synchronization* — or *synch* — *word*. For example all the Galileo I/NAV message pages begin with the sequence 0101100000.

The search process leading to the identification of the starting point of a valid page is called *frame synchronization*. This is generally achieved by the identification of a valid synch word.

The T_{synch} is defined as the time between the epoch at which the first navigation symbol coming from the tracking loop is available and the epoch of the first successful validity check.

Assuming that no bit errors are encountered, the worst case causing the longest waiting time is when the first retrieved navigation symbol is located at point A as shown in **Figure 3**, which is the second bit of the currently processed page.

In this case T_{synch} is equal to the duration of two pages minus one bit, while omitting the processing time to compute the CRC, which can be considered negligible. The relationship between T_{synch} and the symbol rate is given by:

$$T_{synch} = \frac{1}{r_s}\left(2 \cdot L_{Page} - 1\right)$$ (18)

where L_{page} is the number of navigation symbols in one page and r_s is the symbol rate. **Equation 18** clarifies the notion that an increased symbol rate helps to reduce the time needed for the frame synchronization.

We now consider the special case of the frame synchronization procedure for the GPS L1C signal. Its message, called CNAV-2, does not present any synch field because frame synchronization is achieved by overlaying code modulated on the pilot component of the signal.

Navigation Message Architecture and Terminology

All data of interest is contained, together with other parameters, in the navigation message transmitted by satellites in the form of a long bit sequence. Each GNSS has its own terminology for describing these groups of bits and there are also different logical ways to identify one particular group.

We use the terminology of the European Galileo system, for example, the F/NAV and call *page* a sequence of bits whose validity is proven by a cyclic redundancy check (CRC) located at its end. The page represents the smallest block of information where a single bit error would cause the whole block to be considered invalid and therefore discarded.

For the page to be valid, the whole block must be received and decoded. If a receiver starts reading the message one bit after the beginning of the current page, the message is considered invalid, and one has to wait until the page has been completed before retrieving the next page of useful information.

Pages of different types are transmitted sequentially for the duration of one subframe, which identifies the upper logical group of information.

Due to their importance and urgency and unlike some other parameters, such as almanac data, differential corrections or other system parameters, the CED and the GST are regularly transmitted within each subframe at a repetition time given by the subframe length in seconds.

Table 6 shows the repetition interval of CED and GST for some GNSS signals.

As an example, we take the structure depicted in **Figure 2**, which is based on the Galileo I/NAV message. A subframe repeating every 30 seconds is shown. The green pages contain CED, while the grey ones contain the system time information. Note that, while all the four green pages should be retrieved for having valid CED, the GST could be retrieved either from page 5 or 6 without distinction.

Signal	Navigation Message	GST Interval	CED Interval
Galileo E1-B	I/NAV	15 s	30 s
Galileo E5a-I	F/NAV	10 s	50 s
GPS L1 C/A	NAV	6 s	30 s
GPS L1C	CNAV-2	18 s	18 s
GPS L5-I5	CNAV	6 s	24 s

TABLE 6. Repetition intervals of CED and GST for various GNSS signals

Elapsed Time [s]	Page Type	Elapsed Time [s]	Page Type
1	Page 2 – CED (2/4)	16	Page 11
2		17	Page 16
3	Page 4 – CED (4/4)	18	
4		19	Page 15
5		20	
6	Page 6 – GST	21	Page 1 – CED (1/4)
7	Page 7/9	22	
8		23	Page 3 – CED (3/4)
9	Page 8/10	24	
10		25	Page 5 - GST
11	Page 12	26	
12		27	Spare
13	Page 14	28	
14		29	Spare
15	Page 11	30	

FIGURE 2 Example structure of a navigation message subframe (Galileo I/NAV)

This sequence has exactly the same length of one frame, or 1800 symbols, and was chosen such that the correlation with shorter sequences would also allow synchronization. The article by J. Rushanan referenced in Additional Resources shows that a sequence of 100 symbols, transmitted over the course of one second, is enough to definitively identify where the frame starts.

In order to be consistent with the approach used in this work, the values of T_{sync} were computed at the 95 percent confidence level. **Table 7** shows the obtained results.

Because the synchronization time presented in Table 6 can be included in the data read time (discussed in the following section), the synch time makes no explicit contribution to the TTFF, as can be also seen in equations (1), (2) and (3).

Navigation Data Read Time

The time required to read the data, described by the terms $T_{CED+GST}$ and T_{GST}, represents the time needed by the receiver to retrieve the navigation parameters, depending on the start condition.

We can divide the parameters into two groups, the clock and ephemeris parameters (CED) and the GNSS system time (GST) parameters. The former group describes the position of the satellite in its orbit and the satellite clock error, while the latter gives information about the time at which a particular message was sent, an essential reference point for the PRN code ambiguity resolution.

In the case of a cold start, both CED and time information are missing, while for a warm start, the availability of a valid CED allows us to perform the first position fix immediately after reading the send time information.

Signal	Frame Sync Time [s]
Galileo E1-B	1.95
Galileo E5a-I	1.95
GPS L1 C/A	11.72
GPS L1C	1.00
GPS L5-I5	5.86

TABLE 7. Frame synchronization time of various GPS and Galileo signals

We use a cumulative distribution function (CDF) to estimate the value of the data read time with the 95 percent confidence, in order to add it to the estimates of the other TTFF contributions. Because the CDF is the integral of the probability density function (PDF), we must first estimate the PDF — a step that we will return to later.

Reading a GNSS Nav Message

In order to read the navigation message, we must first make a table of the time needed to read both CED and GST, considering all the possible points where the reading process can start.

If the current page contains the parameters required for the first position we consider also the cases where the reading

Reading Epoch	$T_{CED+GST}$ [s]	Reading Epoch	$T_{CED+GST}$ [s]
0	24	16	18
0+	32	17	17
1	31	18	16
2	30	19	15
2+	32	20	14
3	31	20+	32
4	30	21	31
5	29	22	30
6	28	22+	32
7	27	23	31
8	26	24	30
9	25	25	29
10	24	26	28
11	23	27	27
12	22	28	26
13	21	29	25
14	20	30	24
15	19	31	32

TABLE 8. Time to get navigation data from the Galileo I/NAV message for different reading epochs
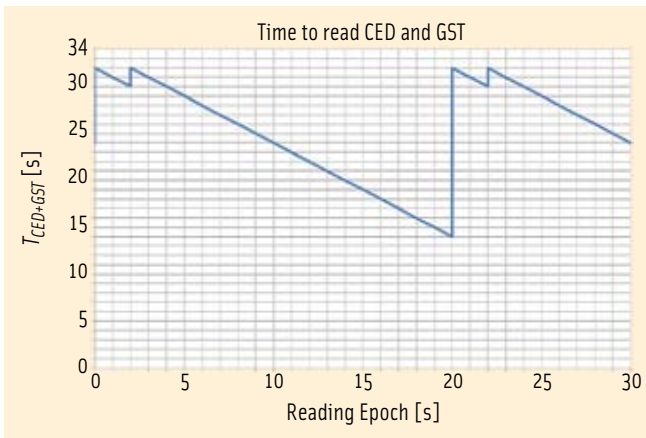
FIGURE 4 Time to read CED and GST from the Galileo I/NAV message as a function of the reaching epochs

point is immediately after the beginning of the page. For a page starting at the time 0, such epoch (implying the loss of the first bits) will be indicated as 0+.

Table 8 shows the $T_{CED+GST}$ values referring to the subframe structure of the Galileo I/NAV message. As we can see, after 30 seconds the time values repeat from the previous subframe.

We plot these values in **Figure 4**, giving us a rough idea of the required reading time versus the reading epoch characteristics.

As one can see, the read time decreases linearly, with discontinuities if the reading epoch is located just after the beginning of a page of interest ($t = 0+$, $t = 2+$, $t = 20+$ and $t = 22+$).

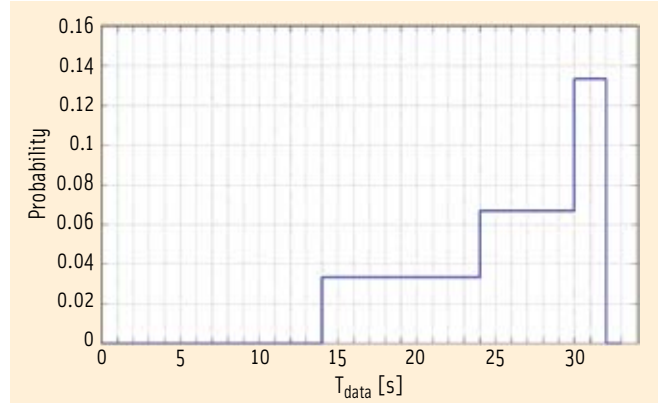The function can be described as follows:

FIGURE 5 Probability density function of the time to read the Galileo I/NAV message

$$\begin{cases} x(t) = 24 & t = 0 \\ x(t) = -t + 32 & 0 < t \leq 2 \\ x(t) = -t + 34 & 2 < t \leq 20 \\ x(t) = -t + 52 & 20 < t \leq 22 \\ x(t) = -t + 54 & 22 < t \leq 30 \end{cases} \tag{19}$$

We now calculate the PDF for $f(t)$ of $T_{CED+GST}$. The entry point in the subframe is assumed to be uniformly distributed over its length in seconds and a count is taken for the frequency with which each possible $T_{CED+GST}$ is observed. By normalizing the occurrences, the searched curve integrates to 1, allowing us to compute the individual probabilities. The results are shown in **Figure 5**.

The mathematical form of the PDF is given by:

$$f(t) = \begin{cases} \dfrac{1}{30} & 14 \leq t \leq 24 \\ \dfrac{1}{15} & 24 \leq t \leq 30 \\ \dfrac{2}{15} & 30 \leq t \leq 32 \\ 0 & \text{elsewhere} \end{cases} \tag{20}$$

At this point the 95 percent probability can be obtained from the following relationship:

$$F(T_{CED+GST}) = \int_{-\infty}^{T_{CED+GST}} f(t)\mathrm{d}t = 0.95 \tag{21}$$

Still referring to this example, we iteratively solve **Equation 21**, obtaining $T_{CED+GST} = 31.63$ seconds as the final result.

This value represents with 95 percent confidence the time needed by the receiver to retrieve the CED and GST parameters from the Galileo I/NAV message. These parameters are necessary for the first position fix, in the case of a cold start.

For the warm start case, only GST needs to be retrieved; the values for the time required to read these data are shown in **Table 9**.

Reading Epoch	T_{GST} [s]
0	6
1	5
2	4
3	3
4	2
4+	22
5	21
6	20
7	19
8	18
9	17
10	16
11	15
12	14
13	13
14	12
15	11

Reading Epoch	T_{GST} [s]
16	10
17	9
18	8
19	7
20	6
21	5
22	4
23	6
24	2
24+	12
25	11
26	10
27	9
28	8
29	7
30	6
31	5

TABLE 9. Galileo I/NAV - Time required to obtain the system time reference for different reading epochs
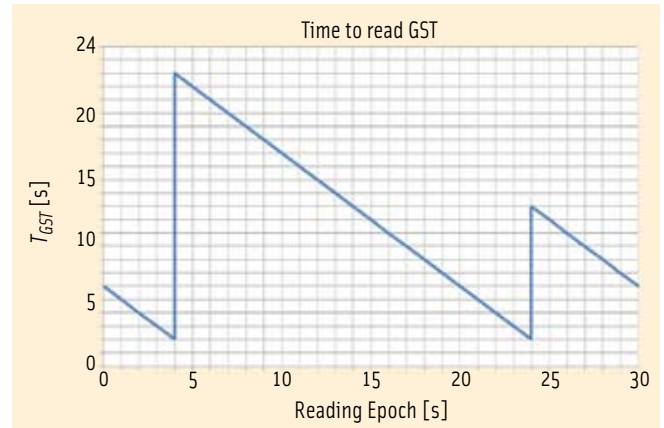

FIGURE 6 Time to read GST from the Galileo I/NAV message as a function of the reading epochs
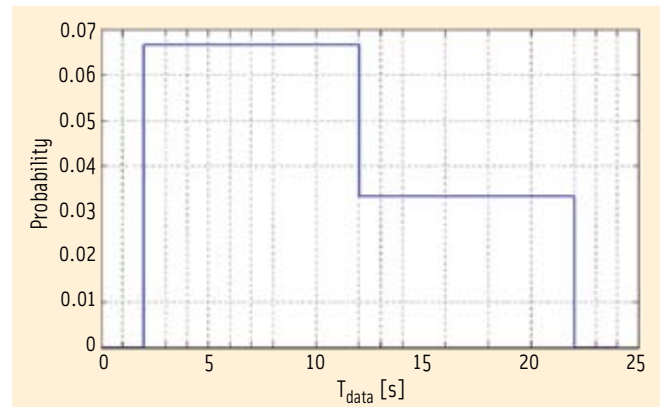
FIGURE 7 PDF of the time to read the GST from the Galileo I/NAV message

Accordingly, the plots of the required time to read the data and of the probability density function change, as presented in **Figure 6** and **Figure 7**.

Also for the warm start case, the 95 percent probability can be obtained by iteration from the cumulative distribution function resulting in T_{GST} = 20.60 seconds.

All these estimates concerning the data read time must be added to the other contributions in order to come up with the overall TTFF estimate.

In **Table 10** we apply this approach to various GNSS signals and report the estimated values for $T_{CED+GST}$ and T_{GST}.

Note that for hot start cases, according to Equation (3), there is no contribution of the data read time.

Key Notes: Navigation Data Delivery Versus Retrieval

At this point we want to underline a few aspects regarding the delivery of the different data messages with respect to the time required to retrieve them.

For the cold start case, a key factor influencing the performance — beside the symbol transmission rate — turns out to be the repetition rate of the CED data. In fact, the GPS L1C (CED every 18 seconds) shows the shortest read time.

A similar consideration applies for the warm start, where the higher repetition rate of the GST information in the GPS signals compensates for the lower symbol transmission rates.

Simulation Results

According to Equations (1), (2), and (3), and substituting the estimates obtained following the approach explained in the previous sections, we come to the final results reported in **Table**

System and Signal	Message	$T_{CED+GST}$ [s] 95% (Cold Start)	T_{GST} [s] 95% (Warm Start)
Galileo E1-B	I/NAV	31.6	20.6
Galileo E5a-I	F/NAV	59.2	37.5
GPS L1 C/A	NAV	35.5	11.7
GPS L1C	CNAV-2	17.6	17.6
GPS L5-I5	CNAV	29.61	11.7

TABLE 10. Estimates of the navigation data read time for different Galileo and GPS messages

11, **Table 12** and **Table 13** for cold, warm, and hot starts, respectively. Note that the time contribution due to acquisition refers to the maximum search strategy.

As can be seen in these three tables, the Galileo E1-B and GPS L5 signals show the best TTFF performance for the cold start case, while for the warm and hot start the GPS L1 C/A code outperforms all other signals.

The very low data rate of the Galileo E5a-I signal results in a quite long data read time and, as a consequence, its TTFF performance is the worst for the cold and warm start cases, where data from the message needs to be retrieved.

For the GPS L1C signal, we can see how the poor performance of the acquisition time, due to the long coherent inte-

System and Signal	$T_{warm-up}$ [s]	T_{acq} [s]	T_{track} [s]	$T_{CED-GST}$ [s]	T_{PVT} [s]	$TTFF_{cold}$ [s]
Galileo E1-B	2.0	2.07	4.8	31.6	2.0	42.47
Galileo E5A-I	2.0	0.26	4.8	59.2	2.0	68.26
GPS L1 C/A	2.0	0.04	4.8	35.5	2.0	44.34
GPS L1C	2.0	41.02	4.8	17.6	2.0	67.42
GPS L5-I5	2.0	0.29	4.8	29.61	2.0	38.70

TABLE 11. Time-to-First-Fix estimates for the receiver cold start

System and Signal	$T_{warm-up}$ [s]	T_{acq} [s]	T_{track} [s]	T_{GST} [s]	T_{PVT} [s]	$TTFF_{cold}$ [s]
Galileo E1-B	2.0	0.92	4.8	20.6	2.0	30.32
Galileo E5A-I	2.0	0.15	4.8	37.5	2.0	46.45
GPS L1 C/A	2.0	0.02	4.8	11.7	2.0	20.52
GPS L1C	2.0	14.62	4.8	17.6	2.0	41.02
GPS L5-I5	2.0	0.16	4.8	11.7	2.0	20.66

TABLE 12. Time-to-first-fix estimates for the receiver warm start

System and Signal	T_{acq} [s]	T_{track} [s]	$TTFF_{hot}$ [s]
Galileo E1-B	0.10	0.5	0.60
Galileo E5A-I	0.03	0.5	0.53
GPS L1 C/A	0.01	0.5	0.51
GPS L1C	1.06	0.5	1.56
GPS L5-I5	0.03	0.5	0.53

TABLE 13. Time-to-first-fix estimates for the receiver hot start

gration and the length of the PRN codes, is counterbalanced by a very short data read time. The GPS L1C signal is, indeed, presenting the shortest data read time because of its particular navigation message structure, which allows for a very short ephemeris repetition time.

Conclusion

We have presented a methodology for the computation of the TTFF for various Galileo and GPS signals while distinguishing the cases of receiver cold, warm, and hot starts. We also considered the main contributions to the TTFF, using simulations, as well as the different acquisition search strategies.

Because the contribution of acquisition time to total TTFF can be substantially decreased by employing new algorithms and technologies, a key factor for a good TTFF performance turns out to be the design of the navigation message structure itself.

The estimates presented in the article were made under the assumption that signals were received with a high enough carrier-to-noise ratio density, such that no bit errors occurred.

We extended our analysis to consider the behavior of the TTFF in low C/N_0 environments. A detailed discussion of these results can be found in the article by M. Paonni et alia (Additional Resources).

Individuals who wish to further investigate the TTFF metric can easily implement our proposed method using GNSS performance simulation tools. We also suggest that this method could be incorporated into GNSS theoretical studies, especially those regarding next-generation systems.

Acknowledgment

Manufacturers

The data presented in this article was plotted using MATLAB from the **Mathworks, Inc.**, Natick, Massachusetts, USA.

Additional Resources

[1] Ávila-Rodríguez J. A., and V. Heiries, T. Pany, and B. Eissfeller, "Theory on Acquisition Algorithms for Indoor Positioning," 12th Saint Petersburg International Conference on Integrated Navigation Systems, Saint Petersburg, Russia, 2005

[2] Borio D., "A Statistical Theory for GNSS Signal Acquisition," (Doctoral Thesis, Politecnico di Torino, Italy, March 2008)

[3] Borio, D., and L. Camoriano, L. Lo Presti, "Impact of the Acquisition Searching Strategy on the Detection and False Alarm Probabilities in a CDMA Receiver," IEEE/ION PLANS 2006, San Diego, CA, USA, 25-27 April 2006

[4] Corazza, G.E., "On the MAX/TC Criterion for Code Acquisition and Its Application to DS_SSMA Systems," *IEEE Transactions on Communications,* Vol. 44, No.9, September 1996

[5] Holmes, J.K., *Spread Spectrum Systems for GNSS and Wireless Communications,* Artech House, 2007

[6] Holmes, J.K., and N. Morgan and P. Dafesh, "A Theoretical Approach to Determining the 95% Probability of TTFF for the P(Y) Code Utilizing Active Code Acquisition," ION GNSS 2006, Fort Worth, Texas, USA, 26-29 September 2006

[7] Mathis, H., and P. Flammant and A. Thiel, "An Analythic Way to Optimize the Detector of a Post-Correlation FFT Acquisition Algorithm," ION GPS/GNSS 2003, Portland, Oregon, USA, September 9-12, 2003

[8] Paonni M., and M. Anghileri, J.-A. Ávila-Rodríguez, S. Wallner, and B. Eissfeller, "Performance Assessment of GNSS Signals in Terms of Time to First Fix for Cold, Warm and Hot Start," *Proceedings of the ION ITM 2010,* January 25-27, 2010, San Diego, California, USA

[9] Polydoros, A., and C.L. Weber, "A unified Approach to Serial Search Spread-Spectrum Code Acquisition – Part I: General Theory," *IEEE Transactions on Communications*, Vol COM-32, No. 5, May 1984

[10] Rushanan, J. J., "The Spreading and Overlay codes for the L1C Signal, *Navigation:* journal of the Institute of Navigation, ISSN 0028-1522 CODEN NAVIB3

[11] Van Dierendonck, A. J., GPS Receivers, in *Global Positioning System: Theory and Applications. Vol. I,* Edited by B.W. Parkinson and J. J. Spilker Jr., Stanford University, USA, 1995

[12] Won, J.-H., "Studies on the Software-Based GPS Receiver and Navigation Algorithms," (Ph.D. diss., Ajou University, December 2004)

[13] Won, J.H., and B. Eissfeller, B. Lankl, Schmitz-Peiffer A., Colzi E., "C-Band User Terminal Con-

cepts and Acquisition Performance Analysis for European GNSS Evolution Programme," ION GNSS 2008, Savannah, GA, USA, September 2008

Authors

"Working Papers" explore the technical and scientific themes that underpin GNSS programs and applications. This regular column is coordinated by **PROF. DR.-ING. GÜNTER HEIN.** Prof. Hein is the head of the European Space Agency's Galileo Operations and Evolution. He was a member of the European Commission's Galileo Signal Task Force and organizer of the annual Munich Satellite Navigation Summit. He has been a full professor and director of the Institute of Geodesy and Navigation at the University of the Federal Armed Forces Munich (University FAF Munich) since 1983. In 2002, he received the United States Institute of Navigation Johannes Kepler Award for sustained and significant contributions to the development of satellite navigation. Hein received his Dipl.-Ing and Dr.-Ing. degrees in geodesy from the University of Darmstadt, Germany. Contact Prof. Hein at <Guenter.Hein@unibw-muenchen.de>

Marco Anghileri is a research associate and Ph.D. candidate at the Institute of Geodesy and Navigation at the University FAF Munich. He studied at the Politecnico di Milano, Italy, and at the Technical University Munich, Germany. He holds an M.Sc .in telecommunication engineering. His scientific research work focuses on GNSS signal structure and on signal-processing algorithms for GNSS receivers.

Matteo Paonni is research associate at the Institute of Geodesy and Navigation at the University of the Federal Armed Forces Munich. He received his M.S. in electrical engineering from the University of Perugia, Italy. He is involved in several European projects with focus on GNSS. His main topics of interest are GNSS signal structure, GNSS interoperability and compatibility, and GNSS performance assessment.

Stefan Wallner studied at the Technical University of Munich and graduated with a Diploma in techno-mathematics. He was research associate at the Institute of Geodesy and

Navigation at the University of the Federal Armed Forces Germany in Munich from 2003 to 2010 and joined the European Space Agency (ESA) just recently. His main topics of interests are spreading codes, the signal structure of Galileo together with radio frequency compatibility of GNSS.

José-Ángel Ávila-Rodríguez is research associate at the Institute of Geodesy and Navigation at the University of the Federal Armed Forces Munich. He is responsible for research activities on GNSS signals, including BOC, BCS, and MBCS modulations. Ávila-Rodríguez is one of the CBOC inventors and has actively participated in the developing innovations of the CBOC multiplexing. He is involved in the Galileo program, in which he supports the European Space Agency, the European Commission, and the European GNSS Supervisory Authority, through the Galileo Signal Task Force. He studied at the Technical Universities of Madrid, Spain, and Vienna, Austria, and has a M.S. in electrical engineering. His major areas of interest include the Galileo signal structure, GNSS receiver design and performance, and Galileo codes. He was recipient of the 2008 Parkinson Award and the 2009 ION Early Achievement Award.

Bernd Eissfeller is a full professor of navigation and director of the Institute of Geodesy and Navigation at the University FAF Munich. He is responsible for teaching and research in navigation and signal processing. Until 1993 he worked in industry as a project manager on the development of GPS/INS navigation systems. He received the Habilitation (venia legendi) in Navigation and Physical Geodesy in 1996 and from 1994–2000 he was head of the GNSS Laboratory of the Institute of Geodesy and Navigation. **IG**